Structural, elastic, electronic and thermodynamic properties of Nd_2Te via first principle calculations

Y. MOGULKOC, Y. O. CIFTCI[a], K. COLAKOGLU[a]
Ankara University, Department of Physics Engineering, Tandogan, Ankara, Turkey
[a]Gazi University, Department of Physics, Teknikokullar, Ankara, Turkey

The structural, elastic, electronic and thermodynamic properties of Nd_2Te compound are investigated using the methods of density functional theory within the generalized gradient approximation (GGA). The thermodynamic property is obtained through the quasi-harmonic Debye model. The results on the basic physical parameters, such as the lattice constant, bulk modulus, pressure derivative of bulk modulus, phase-transition pressure (P_t), second-order elastic constants, Zener anisotropy factor, Poisson's ratio, Young's modulus, and isotropic shear modulus are presented. In order to gain further information, the pressure and temperature- dependent behaviour of the volume, bulk modulus, thermal expansion coefficient, heat capacity, entropy, Debye temperature and Grüneisen parameter are also evaluated over a pressure range of 0 - 15 GPa and a wide temperature range of 0-1200 K.

(Received May 5, 2011; accepted August 10, 2011)

Keywords: Ab-initio, Electronic properties, Thermodynamic properties, Nd_2Te, Plane-wave pseudopotential

1. Introduction

The rare-earth compounds have recently attracted special attention in many applications due to their interesting physical, electronic, and mechanic properties. There is worthy of consideration in multi-component systems based on chalcogenides [1-8].

An interaction of chalcogenides in the Nd_2Te system leads to formation of binary chemical compounds with different formal compositions. In this work we have studied the structural, elastic, electronic and thermodynamic properties of Nd_2Te in C3 (cuprite) and C15 structures using first principle methods using Vienna Ab-initio Simulation Package (VASP).

2. Method of calculation

In this work, all the calculations were carried out using the Vienna Ab initio Simulation Package (VASP) based on the density functional theory (DFT). The electron-ion interaction was taken into consideration in the form of the potential projector-augmented-wave (pot PAW) method [9-12].

The wave functions are expanded in the plane waves up to a kinetic energy cut-off 500 eV. This cut-off energy value was found to be convenient for the electronic band structures and the thermodynamic properties.

The Monkhorst and Pack [13] grid of k-points was used for integration in capable of being reduced part of the Brillouin zone.

We have used the quasi-harmonic Debye model for thermodynamic calculations [14-17]. The quasi-harmonic Debye model has been carried out to calculate the thermodynamic properties of NdTe compounds. The non-equilibrium Gibbs function $G^*(V; P, T)$ can be written as follow [14]:

$$G^*(V;P,T) = E(V) + PV + A_{vib}[\Theta(V);T] \qquad (1)$$

where $E(V)$ is the total energy for per unit cell of Nd_2Te, PV is the constant hydrostatic pressure condition , $\Theta(V)$ is the Debye temperature and A_{vib} is the vibrational Helmholtz free energy which can be written as [18-20]

$$A_{vib}(\Theta,T) = nkT\left[\frac{9\Theta}{8T} + 3\ln\left(1-e^{-\Theta/T}\right) - D(\Theta/T)\right] \qquad (2)$$

where n is the number of atoms per formula unit, $D(\Theta/T)$ describes the Debye integral. The Debye temperature Θ is meant as [20]

$$\Theta = \frac{\hbar}{k}\left[6\pi^2 V^{1/2} n\right]^{1/3} f(\sigma)\sqrt{\frac{B_s}{M}} \qquad (3)$$

where M is the molecular mass per unit cell and B_S is the adiabatic bulk modulus which is approximated given by the static compressibility [14]

$$B_s \approx B(V) = V\left(\frac{d^2E(V)}{dV^2}\right), \qquad (4)$$

$f(\sigma)$ is given by [19, 20]

$$f(\sigma)=\left\{3\left[2\left(\frac{2}{3}\frac{1+\sigma}{1-2\sigma}\right)^{3/2}+\left(\frac{1}{3}\frac{1+\sigma}{1-\sigma}\right)^{3/2}\right]^{-1}\right\}^{1/3} \quad (5)$$

where σ is Poisson ratio. Therefore, the non-equilibrium Gibbs function $G^*(V; P, T)$ as a function of $(V; P, T)$ can be minimized according to volume V as

$$\left[\frac{\partial G^*(V;P,T)}{\partial V}\right]_{P,T}=0\,. \quad (6)$$

The thermal equation-of-state (EOS) $V(P, T)$ can be obtained by solving the equation (6). The isothermal bulk modulus B_T is given by [14]

$$B_T(P,T)=V\left(\frac{\partial^2 G^*(V;P,T)}{\partial V^2}\right)_{P,T}. \quad (7)$$

The thermodynamic quantities, e.g., heat capacities C_V at stable volume and C_P at stable pressure, and entropy S have been calculated by applying the following relations [14]:

$$C_V=3nk\left[4D(\Theta/T)-\frac{3\Theta/T}{e^{\theta/T}-1}\right], \quad (8)$$

$$C_P=C_V(1+\alpha\gamma T), \quad (9)$$

$$S=nk\left[4D(\Theta/T)-3\ln\left(1-e^{-\Theta/T}\right)\right], \quad (10)$$

where α is the thermal expansion coefficient and γ are the Grüneisen parameters which are given by following equations [14]:

$$\alpha=\frac{\gamma C_V}{B_T V}, \quad (11)$$

$$\gamma=-\frac{d\ln\Theta(V)}{d\ln V}. \quad (12)$$

3. Results and discussion

3.1. Structural properties

The calculated equilibrium lattice parameters, bulk modulus and first pressure derivative of bulk modulus for Nd_2Te compound in C3 and C15 structures were computed by minimizing the crystal total energy calculated for different values of lattice constant by means of Murnaghan's equation of state (eos) [21] as in Fig. 1.

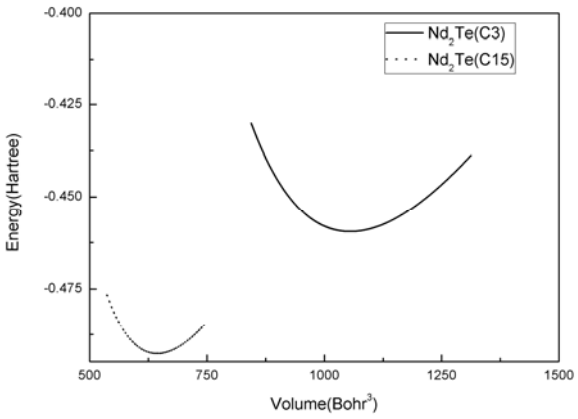

Fig. 1: Total energy versus volume curves of Nd_2Te

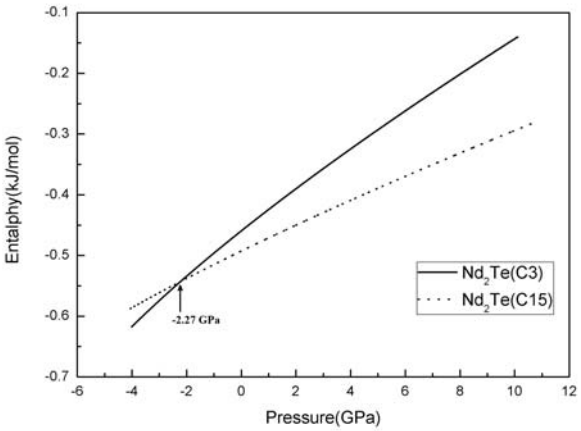

Fig. 2: Transition pressure of Nd_2Te

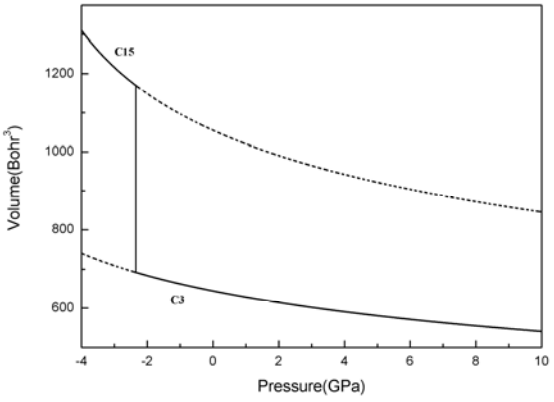

Fig. 3: Pressure versus volume curves of Nd_2Te

Our calculated values of Nd_2Te are presented in Table 1. Also, the bulk modulus and its pressure derivative have been calculated based on the same Murnaghan's equation of state and results are given in Table 1.

Table 1. Calculated equilibrium lattice constant (a_0), bulk modulus (B), the pressure derivative of bulk modulus (B′) and formation entalphy with together the experimental values for Nd_2Te.

Material	Structure	Reference	a_0 [Å]	B [GPa]	B′	Formation Enthalpy
Nd_2Te	C3	Present	6.784	27.78	4.09	-16.23
Nd_2Te	C15	Present	9.127	38.12	4.38	-17.93

The calculated values of formation energy in formula unit are: C3 (-16.23 eV/f.u.) and C15 (-17.93 eV/f.u.) structures for Nd_2Te. These values imply that C15 structure can be synthesized more easily among the considered phases, and the C15 structure is more stable than the C3 one for Nd_2Te compounds.

3.2. Electronic properties

The calculated band structures and corresponding electronic density of state (DOS) of Nd_2Te (C15) phase along the high symmetry directions in the first Brillouin zone are shown in Fig. 4. The position of the Fermi level is set to 0 eV.

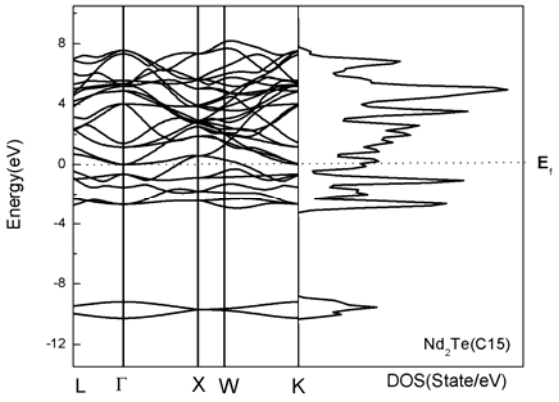

Fig. 4. Calculated energy band structures and DOS of Nd_2Te (C15)

Nd_2Te in C15 exhibits metallic character due to the fact that it is evidently seen from the Fig. 4 that there is no band gap at Fermi energy level (E_F).

3.3. Elastic properties

The elastic constants of solids provide a link between the mechanical and dynamical behaviors of crystals, and give important information concerning the nature of the forces operating in solids. In particular, they provide information on the stability and stiffness of materials. Their first principle calculation requires precise methods since the forces and the elastic constants are functions of the first and second-order derivatives of the potentials.

In this study, stress-strain method [22, 23] was used to obtain the second-order elastic constants (C_{ij}), and the calculated values of elastic constants at zero pressure are listed in Table 2.

Table 2. The calculated elastic constants (in GPa unit) for considered phases of Nd_2Te at zero pressure.

Material	Structure	Reference	C_{11}[GPa]	C_{12}[GPa]	C_{44}[GPa]
Nd_2Te	C3	Present	29.09	28.46	23.92
Nd_2Te	C15	Present	22.69	22.30	18.84

The second-order elastic constants (C_{ij}) are also predicted at various pressures for the most stable phase (C15) of Nd_2Te, and the obtained values are given in Fig. 5. As is expected, both C_{11} and C_{12} increase monotonically with pressure whereas the slope for C_{44}, relatively, is lower. No experimental and the other theoretical data on the pressure-dependence of elastic constants are available in the literature for Nd_2Te for the sake of comparison.

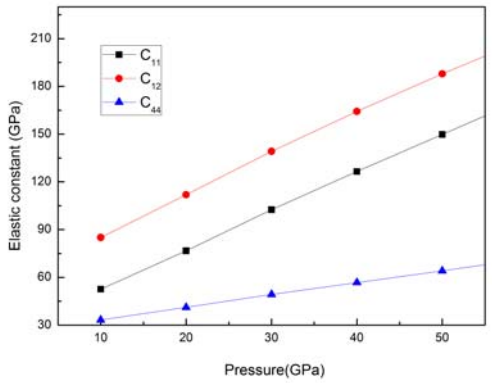

Fig. 5. Calculated second order elastic constants of Nd_2Te (C15)

Table 3. The calculated elastic constants in C15 structure for Nd_2Te at different pressures.

Material	Pressure [GPa]	C_{11} [GPa]	C_{12} [GPa]	C_{44} [GPa]	C' [GPa]
Nd_2Te	10	52.59	85.04	33.24	-16.23
Nd_2Te	20	76.7	111.96	41.16	-17.63
Nd_2Te	30	102.51	139.17	49.27	-18.33
Nd_2Te	40	126.51	164.26	56.75	-18.87
Nd_2Te	50	149.8	187.87	64.13	-19.04

It is seen that the shear modulus increases with increasing pressure values in Table 3.

3.4. Thermodynamic properties

In this section, Debye temperature, melting point, average, transverse and longitudinal sound velocities have been calculated for Nd_2Te system using the following common relations. Debye temperature (θ_D) is calculated from the equation [20].

$$\theta_D = \frac{\hbar}{k}\left[\frac{3n}{4\pi}\left(\frac{N_A\rho}{M}\right)\right]^{1/3} v_m \quad (13)$$

where $\hbar$ is Planck's constant, k is Boltzmann's constant, N_A is Avogadro's number, n is the number of atoms per formula unit, ρ is the density.

Average (v_m), transverse (v_t) and longitudinal (v_l) sound velocities are given [23], respectively, as

$$v_m = \left[\frac{1}{3}\left(\frac{2}{v_t^3} + \frac{1}{v_l^3}\right)\right]^{1/3} \quad (14)$$

$$v_t = \sqrt{\frac{G}{\rho}} \quad (15)$$

$$v_l = \sqrt{\frac{3B+4G}{3\rho}} \ . \quad (16)$$

The melting temperature (T_m) has been calculated using an empirical relation [23],

$$T_m = 553 + (591/\text{Bar})C_{11} \pm 300\text{K}. \quad (17)$$

All calculated quantities from (13-17) are listed in Table 4 for Nd_2Te system.

Table 4. The longitudinal, transverse, and average elastic wave velocity, Debye temperature and melting temperature of Nd_2Te for various phases.

Material	Structure	v_l [m/s]	v_t [m/s]	v_m [m/s]	θ_D [K]	T_m [K]
Nd_2Te	C3	2561.5	1148.4	1295.4	127.6	725 ± 300
Nd_2Te	C15	4540.5	1629.8	1851.6	120.8	687 ± 300

The Nd_2Te (C15) has, relatively, the higher melting point (687±300K) among the considered phases. This value is lower than that for constituent atom Nd (1294K) and for constituent atom Te (722.66K).

Some basic thermo dynamical properties such as bulk modulus, linear thermal expansion coefficient and heat capacity have, also, been investigated under various pressures and temperatures using the quasi-harmonic Debye approximations for Nd_2Te (C15) phases.

The normalized volume and pressure relation is shown in Fig. 6 for Nd_2Te compound. It can be seen that when the pressure increases from 0 GPa to 15 GPa, the volume variation decreases for both of them. The expected volume collapses at phase transition pressure is not seen clearly in this graph. The reason for this changing can be attributed to the atoms in the interlayer that become closer and their interactions become stronger.

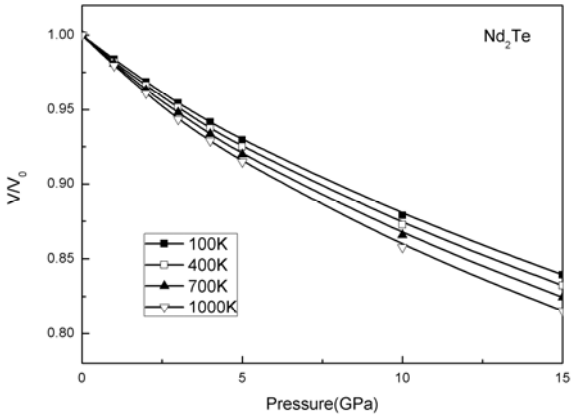

Fig. 6. The normalized volume-pressure diagram for C15 structure of Nd_2Te at 100K, 400K, 700K and 1000K

The variation of the bulk modulus with pressure at different temperatures is shown in Fig. 7. It can be easily seen that as the bulk modulus increases the pressure increases and as the temperature increases, the bulk modulus decreases for both of the compounds.

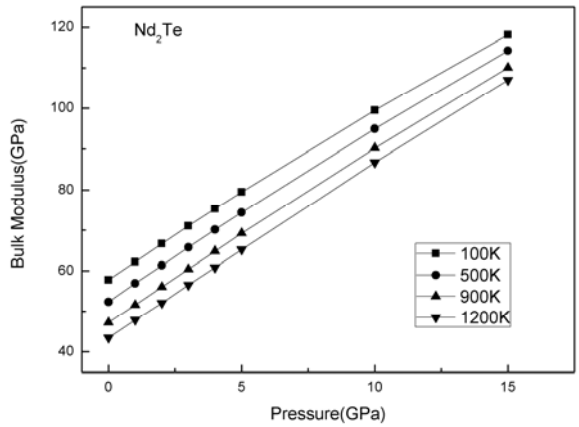

Fig. 7. The bulk modulus-pressure diagram for C15 structure of Nd_2Te.

The variation of bulk modulus (B) with temperatures (T) at 0 GPa is shown in Fig. 8 for C15 phase. As expected, the bulk modulus dramatically decreases as the temperature increases at zero pressure for both phases. Because the lattice parameter, and hence the cell volume increases with the increasing temperature.

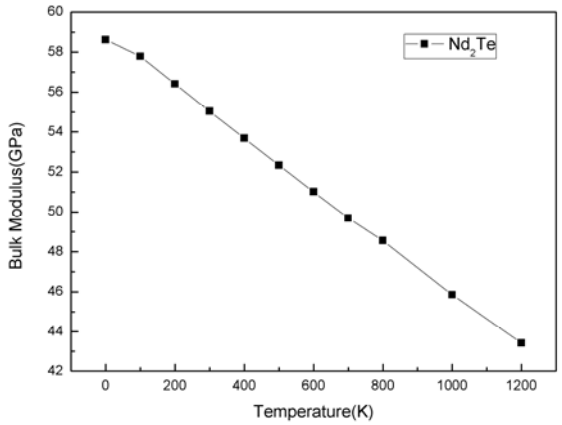

Fig. 8. The variation of bulk modulus (B) with temperatures (T) at 0 GPa for Nd_2Te.

The bulk modulus for Nd_2Te is also fitted data for the temperature-dependent behavior of bulk modulus to a third order polynomial fit:

$B(T)=58.77379-0.011608T-3.116198T^2+1.789357T^3$

The variations of the linear thermal expansion (α) with temperature at different pressures are shown in Fig. 9. The value of α decrease as the pressure increases, at high temperatures. At low temperatures the thermal expansion coefficient increases while pressure decreases in C15 phase.

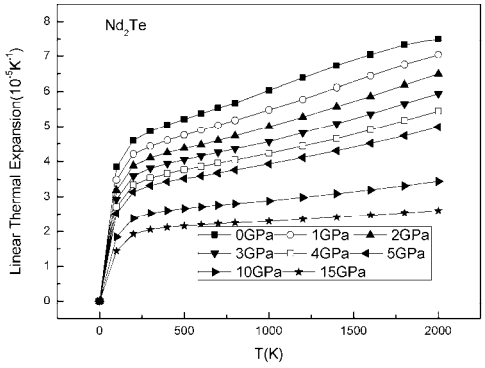

Fig. 9. The linear thermal expansion versus temperature for C15 structure of Nd_2Te.

The temperature dependence of heat capacity (C_v) at various pressures are shown in Fig. 10. It is seen from this figure that when T<300 K, C_v increases very rapidly with temperature; when T> 400 K, C_v increases slowly with temperature and it almost approaches a constant called as Dulong-Petit limit ($C_v(T)$~3R for mono atomic solids) at higher temperatures for Nd_2Te. In addition, this figure implies that the heat capacity is not sensitive to the pressure at high temperature for this compound.

4. Conclusions

In this study, the ab-initio pseudopotential calculations have been performed on the Nd_2Te using the plane-wave pseudopotential approach to the density-functional theory (DFT) within PAW GGA approximation. Our present key results are on the structural, elastic, electronic and thermodynamic properties for Nd_2Te. The electronic band structures with density of states are presented. The calculated structural, elastic and thermodynamic parameters are also given in this text. The calculated formation energy implies that the experimentally most favorable phase is C15. The elastic constants obey the traditional mechanical stability conditions for the considered structures at zero pressure. The electronic band structures and the corresponding density of states showed that the C15 phase is metallic in nature.

References

[1] Chun-Gang Duan, R F Sabirianov, W N Mei, P A Dowben, S S Jaswal and E Y Tsymbal, J. Phys. Condens. Matter **19**, 315220 (2007).
[2] S. Lebegue, A. Svane, M.I. Katsnelson, A.I. Lichenstein and O. Eriksson, Physical Rev. B **74**, 045114 (2006).
[3] Gitanjali Pagare, Sankar P. Sanyal, P.K. Jha, Journal of Alloys and Compounds **398**, 16-20 (2005).
[4] S.Z. Imamalieva, F.M. Sadygov, M.B. Babanly, Inorganic Materials **44**, 935-938 (2008).
[5] W. Lin, H. Steinfink, and E.J. Weiss, Inorganic Chemistry **4**, 877-881(1965).
[6] P. Schobinger-Papamantellost, P. Fischer, A. Niggli, E. Kaldis and V. Hildebrandt, J. Phys. C. Solid State Phys. **7**, 2023 (1974).
[7] Y. Mogulkoc, Y.O. Ciftci, and K. Colakoglu, Fizika, XVI, **2**, 227-230 (2010).
[8] M. Ozayman, Y.O. Ciftci, K. Colakoglu, E. Deligoz, J. Optoelectron. Adv. Mater., **13**, 565-574 (2011).
[9] G. Kresse and J. Hafner, Phys. Rev. B **47**, 558 (1994).
[10] G. Kresse, J. Furthmäuller, Comp. Mat. Sci. **6**, 15 (1996).
[11] G. Kresse and D. Joubert, Phys. Rev. B **59**, 1758 (1999).
[12] G. Kresse and J. Furthmüller, Phys. Rev. B **54**, 11169-1186 (1996).
[13] Hendrik J. Monkhorst and James D. Pack, Phys. Rev. B **13**, 5188 (1976).
[14] M.A. Blanco, E. Francisco,V. Luaña, Comput. Phys. Commun. **158**, 57(2004).
[15] Feng. Peng, Hang-Zhi Fu, Xin-Lu Cheng, Physica B **400**, 83 (2007).
[16] F. Peng, H.Z. Fu, X.D. Yang, Solid State Commun. **145**, 91(2008).
[17] F. Peng, H.Z. Fu, X.D. Yang, Physica B **403**, 2851(2008).
[18] M.A. Blanco, A. Martín Pendás, E. Francisco, J.M. Recio, R. Franco, J. Molec. Struct. (Theochem)

368, 245 (1996).

[19] E. Francisco, J.M. Recio, M.A. Blanco, A. Martín Pendás, A. Costales, J. Phys. Chem. **102**,1595 (1998).
[20] E. Francisco, M.A. Blanco, G. Sanjurjo, Phys. Rev. B **63**, 094107, (2001).
[21] F.D. Murnaghan, Proc. Natl. Acad. Sci. USA **30**, 5390 (1944).
[22] S.Q. Wang, H.Q. Ye, Phys. Stat. Sol.(b) **240**, 45-54 (2003).
[23] E. Screiber, O.L. Anderson and N. Soga Elastic Constants and Their Measurements, 1st edn., New York: McGraw-Hill, (1973).

*Corresponding author: yasemin@gazi.edu.tr